

Singularities in the X-Ray Spectra of Metals*

DAVID C. LANGRETH

Rutgers University, New Brunswick, New Jersey 08903

(Received 4 August 1969)

Recently, Nozières *et al.* have shown that Mahan's model x-ray problem (coupling between the deep hole and electron-hole excitations) could be solved exactly for the singular exponents. Here, it is shown that Lundqvist's model x-ray problem (coupling between the deep hole and plasmons) may also be solved exactly. Furthermore, an exact solution for the singular exponents may be obtained for the more general problem where both effects exist simultaneously. Finally, a perturbation method is developed to treat both effects on an equal footing for a real interacting electron gas.

I. INTRODUCTION

RECENTLY, much progress has been made in the understanding of the singularities in the x-ray absorption and emission spectra of metals. Mahan,¹ Anderson,² and Nozières *et al.*^{3,4} have considered the threshold singularities caused by the coupling of the deep hole with the particle-hole excitations of the electron gas. Lundqvist^{5,6} has, on the other hand, emphasized the importance of the effects of the coupling of the deep hole to the plasma oscillations of the electron gas. Here, we show that: (i) Lundqvist's model problem may be solved exactly with results qualitatively different from his; (ii) if both plasmon and particle-hole coupling to the deep hole is included, the problem may still be solved, essentially, exactly (in the sense of Ref. 3); finally, (iii) a perturbation expansion may be developed to treat both effects on an equal footing for a real interacting electron gas.

Here, we shall consider only model Hamiltonians of the form

$$\mathcal{H} = \epsilon c^\dagger c + c c^\dagger V + H_e, \quad (1)$$

where c is the creation operator for the deep hole of energy ϵ , V represents the interaction between the deep hole and the conduction electrons and involves only conduction-electron coordinates, and H_e is the Hamiltonian for the conduction electrons alone. In using (1), we assume, as in Refs. 1–6, that the deep state is structureless and that all effects giving it a width, lifetime, or extra degrees of freedom are neglected. Of interest for x-ray absorption will be the density of occupied states for $N_+(\omega)$ for the deep level; for emission, the

corresponding function is $N_-(\omega)$, the density of unoccupied deep states. In terms of (1), we may write

$$N_+(\omega) = \int_{-\infty}^{\infty} \frac{dt}{2\pi} e^{i\omega t} \langle \psi_+ | c^\dagger(0) c(t) | \psi_+ \rangle, \quad (2a)$$

$$N_-(\omega) = \int_{-\infty}^{\infty} \frac{dt}{2\pi} e^{i\omega t} \langle \psi_- | c(t) c^\dagger(0) | \psi_- \rangle, \quad (2b)$$

where $c(t) = e^{iHt} c e^{-iHt}$. Here, $|\psi_+\rangle$ is the exact ground state of the no-hole Hamiltonian, that is, it is the product of the state containing no deep holes and the ground-state wave function of H_e . Similarly, $|\psi_-\rangle$ is the exact ground state of the one-hole system, that is, it is the product of the state containing exactly one deep hole and the ground-state wave function of $H_e + V$. Generally, we shall obtain $N_\pm(\omega)$ by calculating the deep Green's function

$$g_\pm(t-t') = -i \langle \psi_\pm | T c(t) c^\dagger(t') | \psi_\pm \rangle. \quad (3)$$

In terms of g , $N_\pm(\omega)$ may be expressed as

$$\pi N_\pm(\omega) = \pm \text{Im} g_\pm(\omega \mp i\eta), \quad (4)$$

where

$$g_\pm(z) = \int_{-\infty}^{\infty} g_\pm(t) e^{izt} dt \quad (5)$$

and where η is a positive infinitesimal. The x-ray absorption will generally be proportional to the convolution of $N_+(\omega)$ with the Fourier transform of the conduction-electron correlation function $\langle c_k(t) c_k(0) \rangle$ provided that this correlation function is calculated in presence of an interaction which is equal to V for times after the x ray as absorbed and before it is re-emitted, but which equals zero otherwise. A similar relation holds for emission involving $N_-(\omega)$. $N_+(\omega)$ will also be important in determining x-ray photoemission and the electron-energy loss spectrum.

II. EFFECT OF PLASMONS

In this section⁷ we adopt Lundqvist's model Hamiltonian

$$\mathcal{H} = \epsilon c^\dagger c + \sum_q c c^\dagger g_q (a_q + a_q^\dagger) + \sum_q \omega_q a_q^\dagger a_q, \quad (6)$$

⁷ Similar techniques have been applied to the optical problem by M. Lax, *J. Chem. Phys.* **20**, 1752 (1952). See also R. P. Feynman, *Phys. Rev.* **84**, 108 (1951).

* Work supported in part by the National Science Foundation, NSF Grant No. GP-14855.

¹ G. D. Mahan, *Phys. Rev.* **153**, 882 (1967); **163**, 612 (1967).

² P. W. Anderson, *Phys. Rev. Letters* **18**, 1049 (1967).

³ R. Roulet, J. Gavoret, and P. Nozières, *Phys. Rev.* **178**, 1072 (1969); P. Nozières, J. Gavoret, and B. Roulet, *ibid.* **178**, 1084 (1969).

⁴ P. Nozières and C. J. De Dominicis, *Phys. Rev.* **178**, 1097 (1969), hereafter abbreviated ND; D. C. Langreth, *ibid.* **182**, 973 (1969).

⁵ B. I. Lundqvist, *Phys. Kondensierten Materie* **9**, 236 (1969).

⁶ The coupling of a conduction electron or hole to the plasmons and its effect on the x-ray spectra has been discussed by a number of workers including R. A. Ferrell, *Phys. Rev.* **107**, 450 (1957); A. J. Glick and P. Longe, *Phys. Rev. Letters* **15**, 589 (1965); L. Hedin, B. I. Lundqvist, and S. Lundqvist, *Solid State Commun.* **5**, 237 (1967); B. I. Lundqvist, *Physik Kondensierten Materie* **6**, 193 (1967); **6**, 206 (1967); **7**, 117 (1968).



FIG. 1. Approximation used by Lundqvist to calculate the self-energy of the deep hole. The double solid line represents the deep Green's function and the wavy line represents the plasmon Green's function.

where a_q^\dagger is the creation operator for a plasmon, $\omega_q = \omega_{-q}$ is the plasmon frequency, and $g_q = g_{-q} = g_q^*$ is the coupling constant between the plasmon and the deep hole. Lundqvist attempted to solve (6) by calculating the self-energy of the deep Green's function in lowest-order perturbation (see Fig. 1). The results are sketched in Fig. 2; the δ -function threshold contribution is reduced and shifted, while the lost spectral density appears as a broad plasmaron peak beginning at a frequency ω_p below the threshold.

Actually, using (6), $N_+(\omega)$ may be calculated exactly. The zero-hole Hamiltonian is just $\sum_q \omega_q a_q^\dagger a_q$, so that $|\psi_+\rangle$ is the state that contains no holes and no plasmons. Hence, according to (2a)

$$2\pi N_+(\omega) = \int_{-\infty}^{\infty} e^{i(\omega-\epsilon)t} \langle 0 | \exp(i\tilde{H}t) | 0 \rangle dt, \quad (7)$$

where $|0\rangle = c|\psi_+\rangle$, and \tilde{H} is the one-hole Hamiltonian

$$\tilde{H} = H_e + V = \sum_q g_q (a_q + a_q^\dagger) + \sum_q \omega_q a_q^\dagger a_q. \quad (8)$$

Since (8) represents a collection of displaced harmonic oscillators, the solution to (7) is imminent. Since $P_q = \frac{1}{2}i(a_q - a_q^\dagger)$ is the momentum conjugate to the displacement $Q_q = a_q + a_q^\dagger$, then $\exp[2if_q P_q]$ is the unitary transform that displaces Q_q an amount $2f_q$. Explicitly, $U a_q U^\dagger = f_q + a_q$, where $U = \exp[\sum_q f_q (a_q - a_q^\dagger)]$, as may be checked using the nested commutator expansion $e^A B e^{-A} = B + [A, B] + \dots$. Picking $f_q = g_q/\omega_q$ diagonalizes \tilde{H} :

$$U \tilde{H} U^\dagger = -\Delta\epsilon + \sum_q \omega_q a_q^\dagger a_q, \quad (9)$$

where

$$\Delta\epsilon = \sum_q g_q^2 / \omega_q. \quad (10)$$

Hence,

$$\begin{aligned} \langle 0 | \exp(i\tilde{H}t) | 0 \rangle &= \langle 0 | U^\dagger \exp[i \sum_q \omega_q a_q^\dagger a_q t] U | 0 \rangle e^{-i\Delta\epsilon t} \\ &= \langle 0 | U^\dagger(0) U(t) | 0 \rangle e^{-i\Delta\epsilon t}, \end{aligned} \quad (11)$$

where

$$\begin{aligned} U(t) &= \exp[i \sum_q \omega_q a_q^\dagger a_q t] U \exp[-i \sum_q \omega_q a_q^\dagger a_q t] \\ &= \exp[\sum_q f_q (a_q e^{-i\omega_q t} - a_q^\dagger e^{i\omega_q t})]. \end{aligned} \quad (12)$$

Substitution back in (7) yields

$$\langle 0 | \exp(i\tilde{H}t) | 0 \rangle = e^{-i\Delta\epsilon t} e^{-\sum_q f_q^2} \exp[\sum_q f_q^2 e^{i\omega_q t}] \quad (13)$$

after making use of the identity $e^{A+B} = e^A e^B e^{-1/2[A,B]}$ several times to move all the destruction operators to

the right. For simplicity at this point, we make the unnecessary assumption that $\omega_q = \omega_p = \text{const}$, that is, we neglect plasmon dispersion. Then

$$2\pi N_+(\omega) = \int dt e^{i(\omega-\epsilon-a\omega_q)t} e^{-a} \exp[ae^{i\omega_q t}], \quad (14)$$

where $a = \sum_q f_q^2 = \omega_p^{-2} \sum_q g_q^2$. The Fourier transform is easily performed by expanding the last exponential to

$$N_+(\omega) = \sum_{n=0}^{\infty} (e^{-a} a^n / n!) \delta(\omega - \epsilon - a\omega_p + n\omega_p). \quad (15)$$

We note that the broad plasmaron peak of second-order perturbation theory is replaced by a series of δ -function peaks in the exact treatment. The weight factor $e^{-a} a^n / n!$ represents the probability that the final state having n real plasmons is contained in the initial state containing no plasmons. This interpretation may be confirmed by carrying out the Fourier transform (7) directly, obtaining

$$\begin{aligned} N_+(\omega) &= \langle 0 | \delta(\omega - \epsilon + \tilde{H}) | 0 \rangle \\ &= \sum_n |\langle 0 | \psi_n \rangle|^2 \delta(\omega - \epsilon - a\omega_p + n\omega_p), \end{aligned} \quad (16)$$

where the $|\psi_n\rangle$ are the exact eigenstates of \tilde{H} , which according to (9) contain n real plasmons in addition to the ground state of \tilde{H} .

The emission spectrum $N_-(\omega)$ may also be easily calculated. Here, $|\psi_-\rangle = U^\dagger |0\rangle$ where $|0\rangle$ contains no plasmons and no deep electrons (one deep hole). Ac-

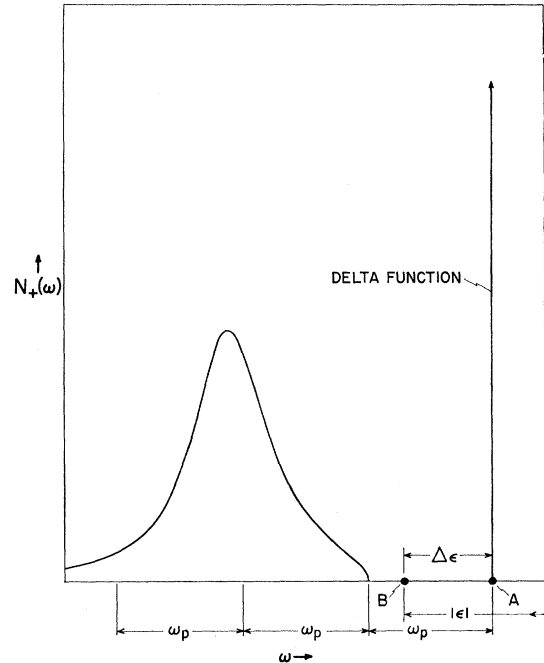


FIG. 2. Deep density of states $N_+(\omega)$ obtained using the approximation of Fig. 1.

cording to (2b), (6), and (9), we have

$$2\pi N_-(\omega) = \int_{-\infty}^{\infty} dt e^{i(\omega - \epsilon - \Delta)t} \langle 0 | U \exp[-i \sum_{\mathbf{q}} \omega_{\mathbf{q}} a_{\mathbf{q}}^\dagger a_{\mathbf{q}} t] U^\dagger | 0 \rangle. \quad (17)$$

Using the same procedures as in the absorption case, we write

$$\langle 0 | U \exp[-i \sum_{\mathbf{q}} \omega_{\mathbf{q}} a_{\mathbf{q}}^\dagger a_{\mathbf{q}} t] U^\dagger | 0 \rangle = \langle 0 | U(t) U^\dagger(0) | 0 \rangle = e^{-a} \exp(ae^{-i\omega t}). \quad (18)$$

Therefore,

$$N_{\pm}(\omega) = \sum_{n=0}^{\infty} (e^{-a} a^n / n!) \delta(\omega - \epsilon - a\omega_p \mp n\omega_p). \quad (19)$$

The probability is that, for emission $e^{-a} a^n / n!$, there are n plasmons bound to the initial deep hole. This interpretation may be confirmed by Fourier transforming (17) directly as

$$N_-(\omega) = \sum_n |\langle \psi_0 | n \rangle|^2 \delta(\omega - \epsilon - a\omega_p + n\omega_p), \quad (20)$$

where $|\psi_0\rangle = U^\dagger | 0 \rangle$ and where all states labeled $|n\rangle$ contain exactly n plasmons.⁸ We note that the emission and absorption spectra for the deep state are similar in that they begin at the same energy $\epsilon + a\omega_p$; however, the plasmon satellites are on the low-energy side of the zero-plasmon peak for absorption, but on the high side for emission. One might also note that for absorption, the first moment $\int d\omega (\omega - \epsilon) N_+(\omega)$ exactly vanishes; this is true for any Hamiltonian of the form in Eq. (1).

III. PARTICLE-HOLE EXCITATIONS AND PLASMON EFFECT

Anderson² has shown that the conduction-electron parts of the zero-deep hole and the one-deep hole wave function are orthogonal for an infinite system (in the presence of an interaction between the deep hole and the conduction electrons), so that the threshold δ function will have zero weight. It is replaced by a power law singularity as shown in detail by Nozières *et al.*^{3,4} One might expect that the plasmon satellites will be similarly modified. Here, we address ourselves to this problem by considering the model Hamiltonian

$$\mathcal{H} = \epsilon c^\dagger c + \sum_{\mathbf{q}} c c^\dagger g_{\mathbf{q}} (a_{\mathbf{q}} + a_{\mathbf{q}}^\dagger) + \sum_{\mathbf{k}\mathbf{k}'\sigma} V_{\mathbf{k}\mathbf{k}'} c_{\mathbf{k}\sigma}^\dagger c_{\mathbf{k}'\sigma} c c^\dagger + \sum_{\mathbf{q}} \omega_{\mathbf{q}} a_{\mathbf{q}}^\dagger a_{\mathbf{q}} + \sum_{\mathbf{k}\sigma} \epsilon_{\mathbf{k}} c_{\mathbf{k}\sigma}^\dagger c_{\mathbf{k}\sigma}, \quad (21)$$

⁸ Since the hole has only one degree of freedom (it does not recoil), there is no correlation between the emission (and reabsorption) of subsequent virtual plasmons. It therefore follows from probability theory that if a is the average number of plasmons surrounding the hole, then the probability that there are exactly n at a given time is given by the Poisson distribution $e^{-a} a^n / n!$.

where $c_{\mathbf{k}\sigma}^\dagger$ is the creation operator for a conduction electron of wave vector \mathbf{k} , spin σ , and energy $\epsilon_{\mathbf{k}}$. The third term causes the Anderson orthogonality block. This Hamiltonian may be solved exactly because the plasmons are taken to be well-defined excitations independent of the pair excitations.

To proceed, we note that now $|\psi_+\rangle$ has no holes, no plasmons, and no pair excitations of the electron gas. Hence,

$$2\pi N_+(\omega) = \int_{-\infty}^{\infty} dt e^{i(\omega - \epsilon)t} \langle 0 | \exp(i\tilde{H}t) | 0 \rangle, \quad (22)$$

where $|0\rangle = c|\psi_0\rangle$ and $\tilde{H} = H' + H''$,

$$H' = \sum_{\mathbf{q}} g_{\mathbf{q}} (a_{\mathbf{q}} + a_{\mathbf{q}}^\dagger) + \sum_{\mathbf{q}} \omega_{\mathbf{q}} a_{\mathbf{q}}^\dagger a_{\mathbf{q}}, \quad (23)$$

$$H'' = \sum_{\mathbf{k}\mathbf{k}'\sigma} V_{\mathbf{k}\mathbf{k}'} c_{\mathbf{k}\sigma}^\dagger c_{\mathbf{k}'\sigma} + \sum_{\mathbf{k}\sigma} \epsilon_{\mathbf{k}} c_{\mathbf{k}\sigma} c_{\mathbf{k}\sigma}^\dagger.$$

Since H' and H'' commute (by assumption), Eq. (22) factors:

$$\langle 0 | e^{iH''t} | 0 \rangle = \langle 0 | e^{iH't} | 0 \rangle \langle 0 | e^{iH''t} | 0 \rangle = \langle 0 | e^{iH''t} | 0 \rangle e^{-ia\omega_p t} e^{-a} \exp(ae^{i\omega_p t}) \equiv e^{C(t)}, \quad (24)$$

where we have used the results of Sec. II. The quantity $\langle 0 | e^{iH''t} | 0 \rangle \equiv e^{C''(t)}$ is precisely the quantity calculated by ND who found that, asymptotically, for large t

$$C''(t) \rightarrow -i\Delta t - \alpha [\ln |Dt| - \frac{1}{2}i\pi \operatorname{sgn} t]. \quad (25)$$

The energy shift Δ and the effective energy cutoff D depend on the details of the potential $V_{\mathbf{k}\mathbf{k}'}$; the exponent α , on the other hand, is determined solely by the phase shifts of $V_{\mathbf{k}\mathbf{k}'}$ at the Fermi level:

$$\alpha = \sum_{l m \sigma} (\delta_{l m \sigma} / \pi)^2. \quad (26)$$

One can similarly extend these results for emission as well, obtaining

$$2\pi N_{\pm}(\omega) = \int_{-\infty}^{\infty} dt e^{i(\omega - \epsilon)t} e^{C_{\pm}(t)}, \quad (27)$$

with

$$C_{\pm}(t) \rightarrow -i(a\omega_p + \Delta)t - a[1 - e^{\pm i\omega_p t}] - \alpha [\ln |Dt| \mp \frac{1}{2}i\pi \operatorname{sgn} t]. \quad (28)$$

As noted by ND, the asymptotic form of $C_{\pm}(t)$ is all that is necessary to obtain the singular parts of $N_{\pm}(\omega)$; the terms linear and oscillatory in t determine the positions of the singularities; the other divergent terms determine the shape of the singularities. From (27) and (28), we find that

$$N_{\pm}(\omega) = \sum_n (e^{-a} a^n / n!) B_{\pm}(\omega - \epsilon - \Delta - a\omega_p \pm n\omega_p), \quad (29)$$

where

$$B_{\pm}(\omega) \propto |\omega|^{-1} \theta(\mp \omega) \quad (30)$$

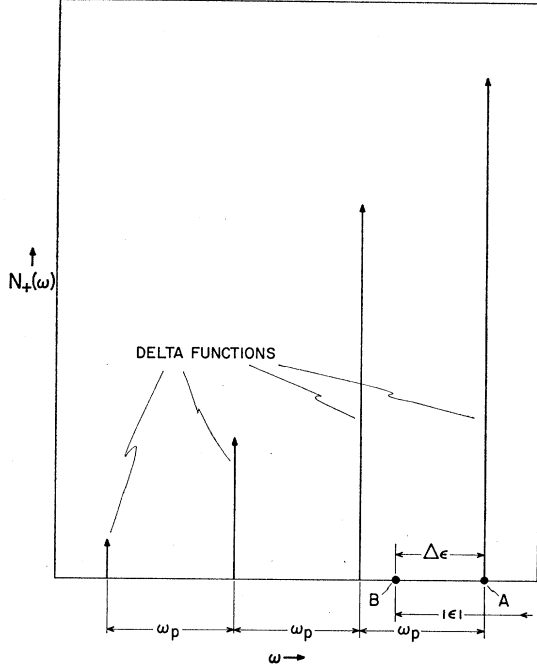


FIG. 3. Exact density of states $N_+(\omega)$ according to the Hamiltonian [see Eq. (6)]. The peaks are shown here decreasing in weight with decreasing ω , but for sufficiently large a ($a > 1$), their weights will increase before decreasing. The center of gravity of the distribution is always $a\omega_p$ to the left of point A, i.e., at point B. The deep state spectra for emission $N_-(\omega)$ is obtained by reflecting the above graph about point A.

near $\omega = 0$. Here, $\theta(x)$ equals zero or 1 for x negative or positive, respectively. Thus, the effect of the interaction with pair excitations is to replace the δ functions of Fig. 3 by B_{\pm} , as shown in Fig. 4. Up to this point we have neglected dispersion, which will soften the singularities of the satellites, but we leave the zero-plasmon singularity intact. Of course, in real materials, the width and lifetime of the deep state would soften the threshold singularity as well.

It should be mentioned that to obtain the actual x-ray emission or absorption spectrum, Eq. (29) must be convoluted with an effective conduction-electron density of states F , which as shown by ND is to be calculated in the presence of the transient potential mentioned earlier. The only point we wish to make here is that F is not affected by the plasmon interaction in (21), although it would be in a more realistic model where the plasmons were allowed to interact directly with the conduction electrons.

IV. PERTURBATION THEORETIC SOLUTION

An obvious weakness of the model Hamiltonian of Sec. III is the assumption that the plasmons are well-defined excitations independent of whatever particle-hole excitations are present. One would like to have a method for calculating the spectrum directly from the properties of the interacting electron gas. A perturbation

theoretic method for this is described in Sec. V. As a prelude, however, we show how the plasmon problem of Sec. II may be solved by summing all the terms in perturbation theory, using a method analogous to ND for the particle-hole problem.

Consider the absorption case first. The diagrams for the deep propagator $ig_+(t-t')$ are of the usual electron-phonon type as shown in Fig. 5. The double solid line represents the bare deep propagator

$$ig_+^{(0)}(t-t') = -\theta(t'-t)e^{-i\epsilon(t-t')}, \quad (31)$$

and the wavy lines represent the plasmon propagator

$$\begin{aligned} i\mathcal{D}_q(t-t') &= \langle \psi_+ | T \phi_q(t) \phi_q^\dagger(t') | \psi_+ \rangle, \\ i\mathcal{D}_q(t) &= D_q(t)\theta(t) + D_q(-t)\theta(-t), \end{aligned} \quad (32)$$

where $\phi_q = a_q + a_{-q}^\dagger$ and $D_q(t) = e^{-i\omega_q t}$. (Note that this is the same as the bare propagator in the absence of interaction. In the emission case, the two are not the same, but we shall use the symbol $\mathcal{D}_q(t)$ for the bare propagator in that case also.) Each solid dot (vertex) receives a factor of $-ig_q$. It is clear that $g_+(t-t')$ vanishes unless $t' > t$ and also that all solid dots in the diagrammatic expansion must have intermediate time variables (between t' and t) in order to yield a nonvanishing contribution. Furthermore, except for the trivial exponential factor, whose only effect is to give an over-all exponential factor to g_+ ; the quantity $-ig_+^{(0)}$ is equal to unity, with the proviso that we order all the times in the sequence in which they appear on paper in a given diagram. Hence, as in the ND case, g may be written

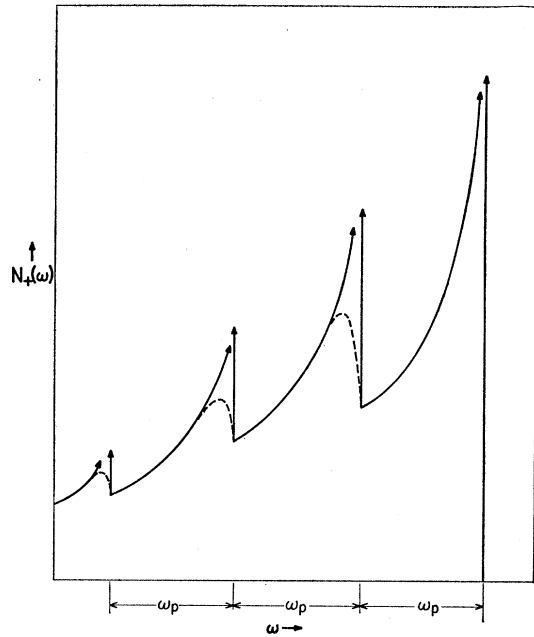


FIG. 4. Deep density of states $N_+(\omega)$ according to Eq. (29). The dashed curves show the effect of plasmon dispersion.

down immediately by the linked-cluster theorem

$$g_+(t-t') = g_+^{(0)}(t-t')e^{C_+(t-t')}, \quad (33)$$

where $C_+(t-t')$ is the sum of the distinct "linked" diagrams, that is, those diagrams which would be linked if the solid $g_+^{(0)}$ lines were removed. There is, of course, only one such diagram, as shown in Fig. 6. Therefore, we have

$$C_+(t-t') = \sum_{\mathbf{q}} (ig_{\mathbf{q}})^2 \int_t^{t'} d\tau \int_t^{t'} d\tau' i\mathcal{D}_{\mathbf{q}}(\tau-\tau')\theta(\tau-\tau')$$

or

$$C_+(t) = -\sum_{\mathbf{q}} g_{\mathbf{q}}^2 \int \frac{d\omega D(\mathbf{q},\omega)(1+i\omega t - e^{i\omega t})}{\omega^2}, \quad (34)$$

where

$$D(\mathbf{q},\omega) = \int_{-\infty}^{\infty} \frac{dt}{2\pi} e^{i\omega t} D_{\mathbf{q}}(t) = \delta(\omega - \omega_{\mathbf{q}}). \quad (35)$$

Equations (33) and (34) are in exact agreement with the results found in Sec. II.

The emission case is slightly more complicated. To preserve the feature that the intermediate times in Fig. 5 be between t and t' we must rewrite the Hamiltonian of Eq. (6) as

$$H = \epsilon c^\dagger c - \sum_{\mathbf{q}} c^\dagger c g_{\mathbf{q}}(a_{\mathbf{q}} + a_{\mathbf{q}}^\dagger) + \sum_{\mathbf{q}} g_{\mathbf{q}}(a_{\mathbf{q}} + a_{\mathbf{q}}^\dagger) + \sum_{\mathbf{q}} \omega_{\mathbf{q}} a_{\mathbf{q}}^\dagger a_{\mathbf{q}}. \quad (36)$$

The third term in (36) will now generate a new set of diagrams shown in Fig. 7. The diagrams in Fig. 5 are evaluated in the same way as for absorption except that now

$$ig_-^{(0)}(t-t') = \theta(t-t')e^{-ie(t-t')}, \quad (37)$$

and the solid dots are now integrated from t' to t . The same rules apply to the diagrams of Fig. 7 except that, in addition, the crosses receive a factor of $+ig_{\mathbf{q}}$ and are integrated from $-\infty$ to ∞ .

The same linked-cluster theorem applies, except now there are two distinct linked diagrams, as shown in Fig.

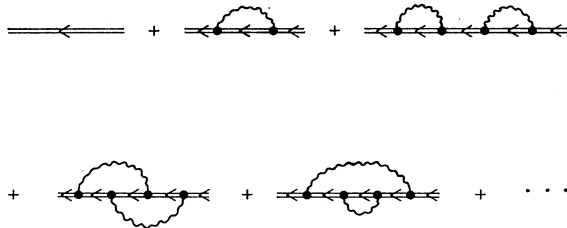


FIG. 5. Diagrammatic series for ig_+ . The same expansion contributes to ig_- , except that here there are additional diagrams, as shown in Fig. 7.



FIG. 6. The only "linked" diagram for $C_+(t-t')$. Note that $t' > \tau' > \tau > t$.

8. The contribution to C from Fig. 8(a) is

$$C_-^{(a)}(t-t') = \sum_{\mathbf{q}} (-ig_{\mathbf{q}})^2 \int_t^{t'} d\tau \int_t^{t'} d\tau' i\mathcal{D}_{\mathbf{q}}(\tau-\tau')\theta(\tau-\tau') \quad (38a)$$

or

$$C_-^{(a)}(t) = -\sum_{\mathbf{q}} g_{\mathbf{q}}^2 \int \frac{d\omega D(\mathbf{q},\omega)(1-i\omega t - e^{-i\omega t})}{\omega^2}. \quad (38b)$$

Similarly, the contribution from Fig. 8(b) is

$$C_-^{(b)}(t-t') = \sum_{\mathbf{q}} (-ig_{\mathbf{q}})(+ig_{\mathbf{q}}) \int_t^{t'} d\tau \int_{-\infty}^{\infty} d\tau' i\mathcal{D}_{\mathbf{q}}(\tau-\tau') \quad (39a)$$

or

$$C_-^{(b)}(t) = -\sum_{\mathbf{q}} g_{\mathbf{q}}^2 \int \frac{d\omega D(\mathbf{q},\omega)(2i\omega t)}{\omega^2}. \quad (39b)$$

Hence, we can summarize the results for both emission and absorption as

$$C_{\pm}(t) = -\sum_{\mathbf{q}} g_{\mathbf{q}}^2 \int_{-\infty}^{\infty} \frac{d\omega D(\mathbf{q},\omega)(1+i\omega t - e^{\pm i\omega t})}{\omega^2}, \quad (40)$$

which is in complete agreement with the results of Sec. II, since $D(\mathbf{q},\omega) = \delta(\omega - \omega_{\mathbf{q}})$.

V. INTERACTION WITH ELECTRON GAS

In this part we apply the methods of Sec. IV to the more realistic case where the deep hole interacts with a fully interacting electron gas. Thus, we again use the Hamiltonian of Eq. (1), but with H_e the interacting

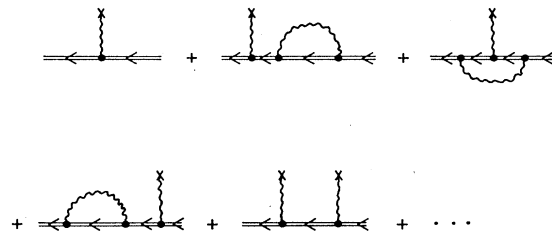


FIG. 7. Extra series of diagrams which contribute to $C_-(t-t')$ but do not contribute to $C_+(t-t')$.

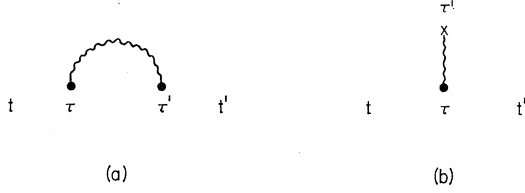


FIG. 8. Two distinct "linked" diagrams for $C_-(t-t')$. Note that $t > \tau > \tau' > t'$ in (a), but that $t > \tau > t'$ and $\infty > \tau' > -\infty$ in (b).

electron gas Hamiltonian, and

$$V = \sum_{\mathbf{q}} V_{\mathbf{q}} \rho_{\mathbf{q}}, \quad (41)$$

where $\rho_{\mathbf{q}}$ is the \mathbf{q} th Fourier component of the conduction-electron density, and $V_{\mathbf{q}}$ is the interaction potential. The diagrams for g_{\pm} are, of course, the usual ones for an external particle interacting with an electron gas. As in Sec. IV, one uses the linked-cluster theorem, except now there are an infinite number of linked diagrams for C . Some of these are illustrated in Fig. 9.

The rules for calculating $C_{\pm}(t-t')$ are as follows: For each conduction-electron line associate a factor $iG_{\mathbf{k}\sigma}^{(0)}(t-t')$, where $G_{\mathbf{k}\sigma}^{(0)}(t-t')$ is the bare propagator for a conduction electron of wave vector \mathbf{k} and spin σ ; for each dashed line associate a factor $-i(4\pi e^2/q^2)$; for each dot associate a factor $\pm iV_{\mathbf{q}}$, and for each cross associate a factor $-iV_{\mathbf{q}}$ for emission, but do not include crosses for absorption; integrate crosses and dashed lines from times $-\infty$ to ∞ ; integrate dots from t to t' for absorption and from t' to t for emission; conserve momentum and spin at Coulomb vertices in the usual way, and give a factor of -1 for each closed G loop.⁹ Finally, g is determined by

$$g_{\pm}(t-t') = g_{\pm}^{(0)}(t-t') e^{C_{\pm}(t-t')}, \quad (42)$$

where C is the diagrammatic sum above and

$$ig_{\pm}^{(0)}(t) = \mp \theta(\mp t) e^{-ie t}. \quad (43)$$

The simplest viable approximation is to treat $V_{\mathbf{q}}$ only to second order, that is to include only those diagrams of the type shown in Fig. 10. In this case, C_{\pm} may be written down, by inspection, in analogy with Eq. (40) as

$$C_{\pm}(t) = -\sum_{\mathbf{q}} |V_{\mathbf{q}}|^2 \int_{-\infty}^{\infty} d\omega S(\mathbf{q}, \omega) \times (1 + i\omega t - e^{\pm i\omega t})/\omega^2, \quad (44)$$

where $S(\mathbf{q}, \omega)$ is the dynamic form factor for the electron gas, that is,

$$S(\mathbf{q}, \omega) = \int \frac{dt}{2\pi} e^{i\omega t} \langle \rho_{\mathbf{q}}(t) \rho_{\mathbf{q}}^{\dagger}(0) \rangle. \quad (45)$$

⁹ Each diagram receives the usual combinatorial factor: A diagram of n_l Coulomb lines, n_d dots, and n_c crosses is to be divided by $n_l! n_d! n_c! 2^{n_l}$ and multiplied by the number of ways the $2n_l + n_d + n_c$ vertices can be connected with G lines to form that particular diagram. In the general case, the method of coupling-constant integration provides a more convenient way of keeping track of these combinatorial factors.

It may also be written as

$$S(\mathbf{q}, \omega) = \frac{q^2}{4\pi^2 e^2} \frac{\epsilon_2(\mathbf{q}, \omega)}{|\epsilon(\mathbf{q}, \omega)|^2} \theta(\omega), \quad (46)$$

where $\epsilon(\mathbf{q}, \omega) = \epsilon_1(\mathbf{q}, \omega) + i\epsilon_2(\mathbf{q}, \omega)$ is the dielectric function of the electron gas.

To see how things go, we use the Lindhard value¹⁰ of ϵ in (46), which has the form (for $\omega > 0$)

$$\begin{aligned} \epsilon_2(\mathbf{q}, \omega) &= E_A(\mathbf{q}, \omega), \text{ for } \omega + q^2/2m < qv_F \\ &= E_B(\mathbf{q}, \omega), \text{ for } |\omega - q^2/2m| < qv_F < \omega + q^2/2m \\ &= 0, \text{ for } qv_F > |\omega - q^2/2m|. \end{aligned} \quad (47)$$

E_A and E_B both contribute to the energy shift Δ and to the energy cutoff D . However, only E_A contributes to the logarithmically divergent term. This is because the integral involving E_B in (44) is perfectly convergent for *each term alone*, so that the first term will give a constant, the second will give an energy times (it), and the third will give a function of t well behaved as $t \rightarrow \infty$. Therefore, so far as the threshold behavior is concerned, only the term involving E_A will be important. E_A is given by

$$E_A(\mathbf{q}, \omega) = (\frac{1}{2}\pi)(\omega/qv_F)(\lambda^2/q^2), \quad (48)$$

where v_F is the Fermi velocity and λ is the Thomas-Fermi wave vector, so that this contribution to C is¹¹

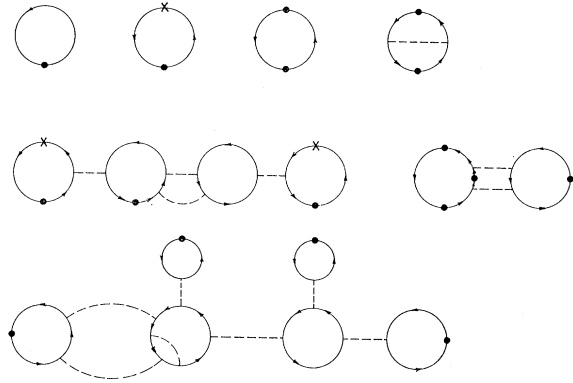


FIG. 9. Typical diagrams contributing to C for the interacting electron gas. Diagrams with crosses contribute only to the emission case. All diagrams have at least one dot. The long-range part of diagram with one dot and no crosses is cancelled by the interaction of the hole with the other ions. Generally the effect of such diagrams is included in the definition of ϵ , so they are omitted.

¹⁰ J. Lindhard, Kgl. Danske Videnskab. Selskab, Mat.-Fys. Medd. **28**, 8 (1954).

¹¹ The fact that the two terms in the integral in Eq. (41) do not individually converge is a manifestation of the Anderson orthogonality block. In fact, the exponential of the first term alone is the weighting factor for the "zero quasiparticle line." For a finite system of volume V , the lower limit would not be zero, but rather would equal the minimum excitation energy of a particle-hole pair $\propto V^{-1/3}$. Hence, this zero quasiparticle weighting factor is $\propto \exp[\alpha \ln V^{-1/3}] = V^{-\alpha/3}$ in agreement with Anderson's results [see Eqs. (44) and (46)].

$$- \sum_{q < 2q_F} |V_q|^2 N(0) \int_0^{\omega_m} \frac{1}{|\epsilon(q, \omega)|^2} \frac{\omega}{qv_F} \times (1 - e^{i\omega t}) / \omega^2 d\omega, \quad (49)$$

where $N(0)$ is the density of states at the Fermi level, and $\omega_m = qv_F - q^2/2m$. We have omitted the $i\omega t$ term in the square brackets, since it just leads to an energy shift and is therefore uninteresting. Equation (49) may be written as ($x = \omega t$)

$$- \sum_{q < 2q_F} |V_q|^2 \frac{N(0)}{qv_F} \int_0^{\omega_m t} \frac{1 - e^{\pm ix}}{x} \frac{1}{|\epsilon[q, (x/t)]|^2} dx. \quad (50)$$

Asymptotically as $|t| \rightarrow \infty$, Eq. (50) becomes

$$-[\alpha \ln(t) + b], \quad (51)$$

where

$$\alpha = \sum_{q < 2q_F} \frac{|V_q|^2}{|\epsilon(q, 0)|^2} \frac{N(0)}{qv_F} \quad (52)$$

and

$$\text{Im} b = \mp \alpha \int_0^{(\text{sgn } t)\infty} \frac{\sin x}{x} dx = \mp \frac{\pi}{2} \text{sgn } t. \quad (53)$$

The real part of b contributes to the effective energy cutoff D , but does not affect the phase of the logarithm. There are other contributions to D from the E_B term. Finally, we note that (52) is the Born approximation for the phase-shift sum

$$\alpha = \sum_{lm\sigma} (\delta_{lm\sigma}/\pi)^2, \quad (54)$$

where the $\delta_{lm\sigma}$'s are to be calculated with the shielded potential $V_q/\epsilon(q, 0)$.

The other contribution to C arises from the zeros of the denominator of (46). Neglecting plasmon dispersion

$$S_{\text{plasmon}}(\mathbf{q}, \omega) \simeq \omega_p(q^2/8\pi e^2) \delta(\omega - \omega_p), \quad (55)$$

for say $q \lesssim \omega_p/v_F \sim q_c$. The plasmon contribution to C is therefore,

$$- \sum_{q < q_c} |V_q|^2 \int_0^\infty \frac{d\omega}{\omega^2} (1 + i\omega t - e^{\pm i\omega t}) \frac{q^2}{8\pi e^2} \omega_p \delta(\omega - \omega_p). \quad (56)$$

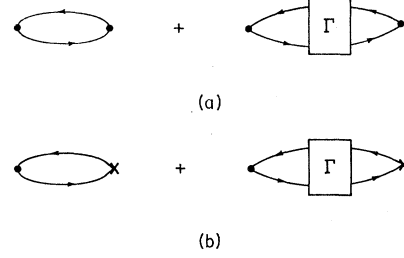


FIG. 10. All the diagrams which contribute to C when V_q is treated in second-order perturbation theory. Diagrams (a) contribute to both absorption and emission, while diagrams (b) contribute only to emission. Here Γ is the complete four-point function for the electron gas. In this figure, the solid- G lines represent the full interacting propagator.

Combining (51) and (56) gives an expression of the form

$$C_{\pm}(t) = -i\Delta t - a[1 - e^{\pm i\omega_p t}] - \alpha[\ln|Dt| \mp i\frac{1}{2}\pi \text{sgn } t], \quad (57)$$

which is the same as (28), although now we have an explicit prescription for calculating the constants. In addition, one could calculate the whole spectrum from (44), which, due to our general arguments, should not differ qualitatively from Fig. 4.

The Friedel sum rule suggests that the use of second-order perturbation theory in V_q may not be too good. It should be interesting to investigate higher-order effects which include the modification of the effective plasmon coupling constant and the plasmon propagator by the transient potential. It should also be interesting to investigate the cancellation effects (Glick and Longe⁶) which arises from plasmon vertex corrections.

Note added in proof. I thank B. Lundqvist for pointing out that plasmon dispersion was included in the theoretical calculation plotted in Fig. 2. Plasmon dispersion has been included numerically in the present theory by L. Hedin, B. Lundqvist, and S. Lundqvist, Proceedings of the National Bureau of Standards Conference on Density of States, 1969 (to be published). Thus, a more accurate comparison of the exact and approximate theories is to be found in this latter work.

ACKNOWLEDGMENTS

I am very grateful to J. W. Wilkins for informing me of the work of Ref. 5, and for helpful and stimulating discussions on this and other matters. I thank the staff of the Physics Department at Cornell, where the finishing touches were put on this paper, for their kindness and hospitality.